Iraqi Journal of Physics, 2026
https://doi.org/10.30723/ijp.v24i2.1411
Vol.24, No.2, PP.96-104
P-ISSN: 2070-4003
E-ISSN: 2664-5548

Light Generation from PbI_2 Nanoparticles Illuminated by a UV Source

Shahad J. Abdul Sahib[1*] and Omar A. Ibrahim[1]
[1]*Department of Physics, College of Science, University of Baghdad, Baghdad, Iraq*
[*]Corresponding author: shahad.abd2304@sc.uobaghdad.edu.iq

Abstract
This study investigates the photoluminescence properties of lead iodide (PbI_2) nanoparticles embedded in a polyvinyl alcohol (PVA) matrix when illuminated by ultraviolet (UV) light. The PbI_2 nanoparticles, dispersed uniformly within the PVA polymer matrix, exhibit enhanced stability and efficient light emission due to the protective environment provided by PVA. Upon UV illumination, the PbI_2 nanoparticles generate visible light, with emission characteristics influenced by the nanoparticle size, concentration, and interaction with the PVA matrix. The role of PVA as a stabilizing agent and its effect on the photophysical properties of PbI_2 are analyzed, showing an improvement in quantum efficiency and photostability. This hybrid nanocomposite system demonstrates potential applications in UV-responsive optoelectronic devices, flexible light-emitting materials, and photonic sensors. The study offers ideas about the integration of semiconductor nanoparticles with polymer matrices for advanced light-generation technologies. This study explores the interaction between UV light and PbI_2 nanoparticles, focusing on the photophysical processes that lead to light generation.

Article Info.

Keywords:
Nanoparticles, Photoluminescence, PbI_2, PVA, Optical Properties.

Article history:
Received: Dec. 19, 2024
Revised: Mar. 21, 2025
Accepted: Apr. 06, 2025
Published:Jun. 01,2026

1. Introduction
Light generation has been studied because light is one of the most important physical phenomena that plays a major role in our daily lives and modern technological applications. When lead halide devices are manufactured using nanotechnology, a noticeable increase in the intensity of generated light is observed. Therefore, these materials have become essential in manufacturing and technology [1-8]. Lead iodide (PbI_2) is a member of the lead halide family, and it is the best in light generation among them, according to the National Renewable Energy Laboratory (NREL). Its power conversion efficiency is in the order of 20.1 % [7, 9]. Therefore, it is important in many applications like photovoltaic conversion, water splitting, light-emitting diodes (LEDs), and tunable electrically pumped lasers [7,10]. In a previous study, the preparation, structural and optical properties of PbI_2 were investigated [11]. The structural properties of the samples were investigated using X-ray diffraction (XRD) to identify the crystalline phase and lattice parameters, as well as scanning electron microscopy (SEM) to examine the surface morphology and grain size. The PbI_2 thin film was tested using Fourier transform infrared spectroscopy (FTIR) and atomic force microscopy (AFM). The optical properties were studied using UV-visible spectroscopy, where absorption and transmittance were measured after depositing PbI_2 on a glass substrate. The evaluated energy gap was 2.3 eV. In this paper, the light generation from nano PbI_2 is studied in order to utilize it for manufacturing optical devices.

2. Materials and Methods
2.1. Preparation of PbI_2: PVA Thin Film
Lead iodide nanoparticles (PbI_2 NPs) were prepared according to the procedure described by Khalaph et al. [12]. PbI_2 was synthesized by reacting aqueous lead nitrate ($Pb(NO_3)_2$) with aqueous potassium iodide (KI) with a molar ratio of 1:3 at room temperature. A yellow precipitate was formed, indicating the creation of PbI_2, as shown in Fig. 1A. The prepared material was centrifuged at a speed of 4000 rpm for 20 minutes. The supernatant was discarded, and the precipitant was dissolved in water and re-centrifuged to remove uninvolved materials. The process

was repeated three times and the precipitate lead iodide was collected. The chemical equation for the reaction is represented by Eq. (1):

$$2KI + Pb(NO_3)_2 \rightarrow PbI_2 \downarrow + 2KNO_3 \quad (1)$$

To prepare the PbI_2: PVA thin films, the PVA polymer solution was first prepared by dissolving 1 g of PVA (supplied by Sigma company) in 20 mL of distilled water. The PbI_2: PVA thin films were then prepared by mixing 1 mL of the PVA polymer solution with 0.05 g of the prepared lead iodide and deposited onto glass plates using the spin coating method at a speed of 1000 rpm for 30 seconds, as shown in Fig. 1C. Additionally, samples were prepared by pouring the mixture into plastic molds and left to dry, as shown in Fig.1B; the prepared samples were then oven-dried at 60°C. It has obtained pure lead iodide, and then the polymer was added to obtain a film, as shown in Fig. 1. It was noticed that the samples emitted green color radiation when irradiated with ultraviolet radiation, as shown in Fig. 2. This emission was studied and analyzed, as it is considered the fundamental component in light generation.

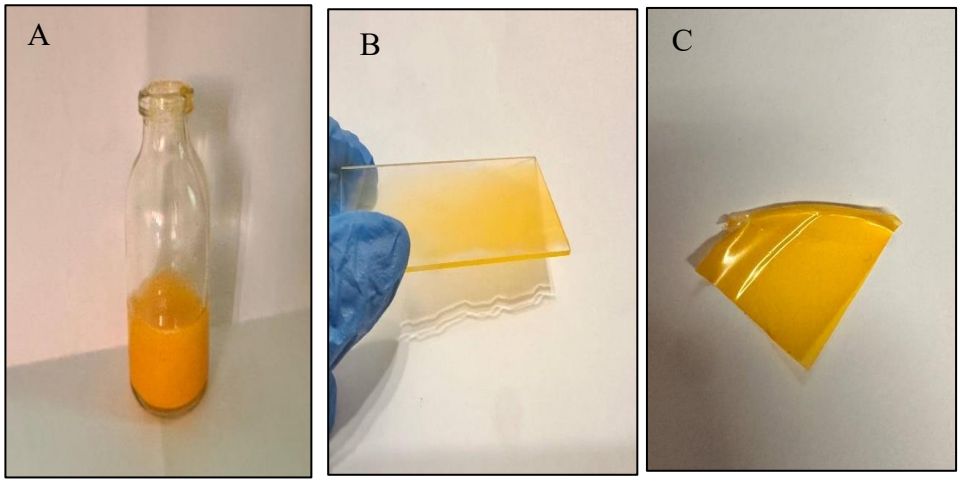

Figure 1: Image of PbI_2: PVA normal light effect.

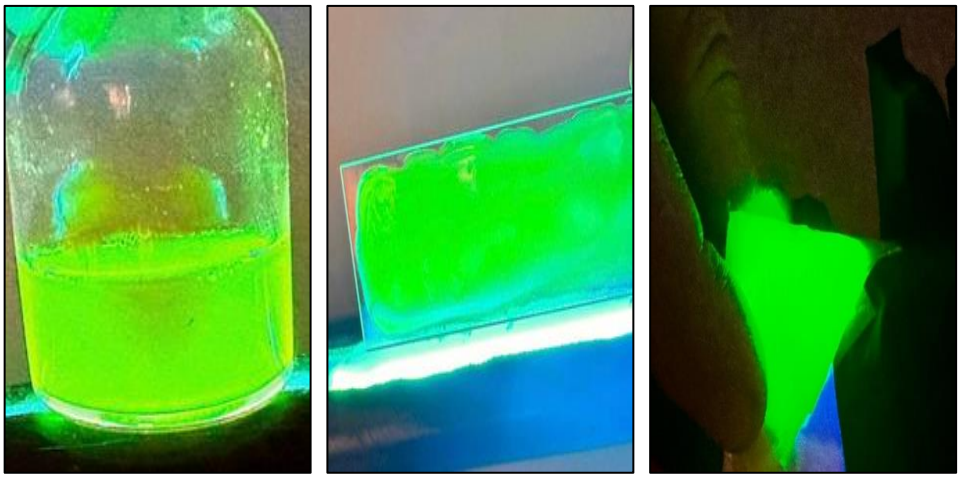

Figure 2: Image of PbI_2: PVA under UV light effect.

2.2. Optical Properties

The optical properties of the prepared PbI_2 nanoparticles were studied employing Photoluminescence (PL) and UV-Vis spectroscopy [13,14].

3. Results and Discussion

3.1. UV-Vis Absorption Spectrum

UV-Vis absorption spectroscopy is an effective method for studying the optical characteristics of lead iodide PbI_2: PVA. Fig. 3 depicts the absorption spectrum of PbI_2 NPs:PVA as a function of wavelength in the range of 280-730 nm. Fig. 3 clearly shows that PbI_2 NPs exhibited very high absorbance in the UV region, which decreased exponentially with increasing wavelength; this indicates that PbI_2 NPs have a high optical response.

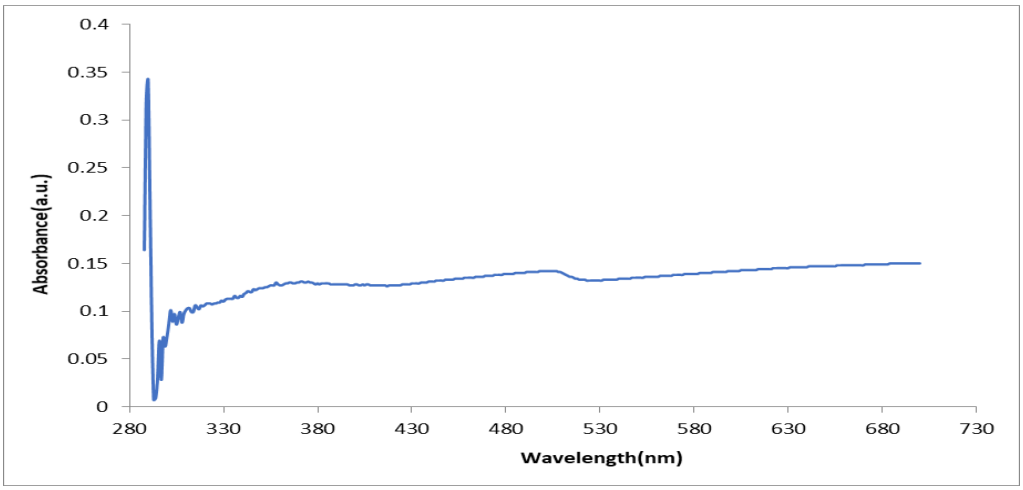

Figure 3: UV-Vis absorption spectrum of PbI_2 NPs: PVA thin film.

The energy band gap of PbI_2: PVA blend was measured using the absorption method. It was computed from the absorbance spectrum using the Tauc relation, according to Eq. (2), as shown in Fig. 4.

$$\alpha h\nu = B\,(h\nu - E_g)^r \qquad (2)$$

It was found that the energy gap was 4.17 eV. Here, indirect electron transfer is forbidden, as shown in Fig. 4. The energy gap measured by the absorption method was larger than that measured by the emission method. Specifically, the energy gap was approximately 4.17 eV in the absorption measurement, whereas it was around 2.8 eV in the emission spectrum. This difference in energy is due to the fact that the transfer is indirect and forbidden, meaning it requires a higher energy to transfer, while emission requires less energy to be emitted.

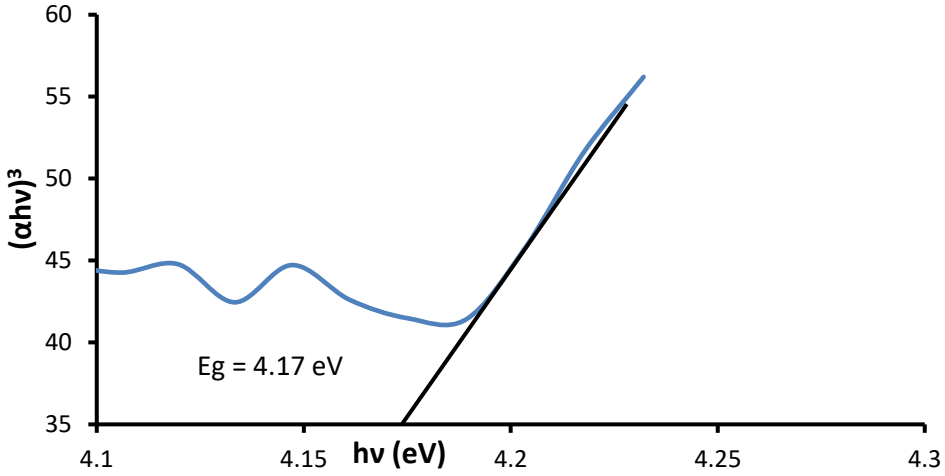

Figure 4: Tauc plot to compute the energy gap of lead Iodide (PbI_2) thin film.

PVA is naturally transparent and usually does not intensely absorb light in the visible range. However, absorption may occur in the ultraviolet range due to the hydroxyl (OH) groups in the polymer structure. When nanomaterials are added, the absorption properties may change due to modifications in the electronic structure of the polymer, as shown in Fig. 5.

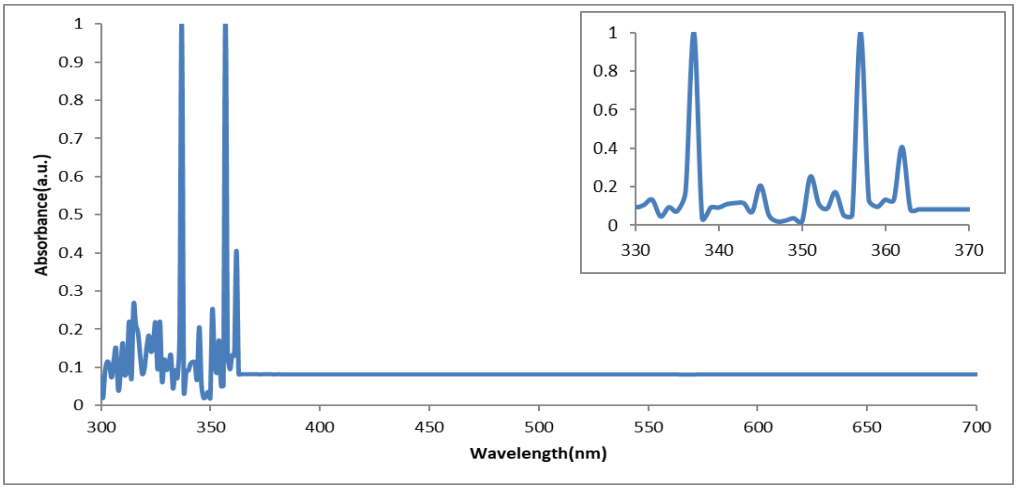

Figure 5: UV-Vis absorption spectrum of PVA.

3.2. Photoluminescence Study (PL)

Photoluminescence spectroscopy provides information about the energy states between the valence and the conduction bands, which are responsible for radiative transitions. This technique was applied to the PbI_2: PVA nanocrystal solution (PbI_2 with a concentration of 2 mol/L) and the wavelength excitation of 290 nm, as shown in Fig. 6.

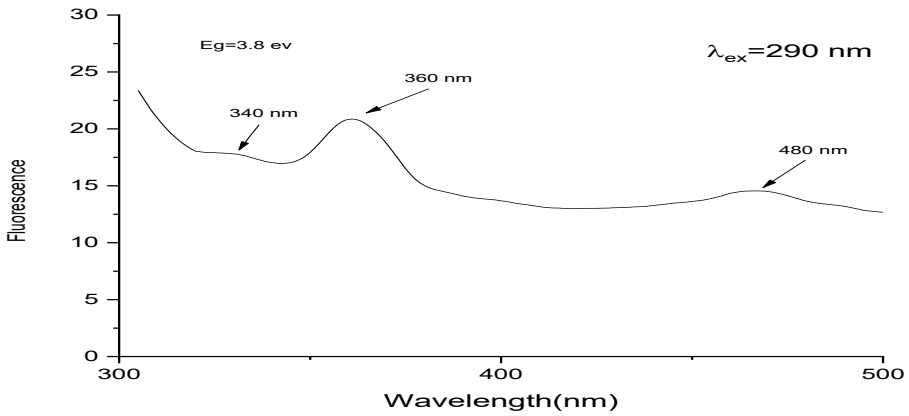

Figure 6: The PL spectrum of PbI_2 NPs: PVA thin film.

After irradiating the material with a wavelength of 290 nm, a set of peaks was obtained, as shown in Fig. 6. It was observed that the peaks at 340 and 360 nm are weak, while the peak at 480nm is broad. Usually, the value of the direct band gap is determined from the photoluminescence peaks using the following Eq. (3):

$$\mathrm{E\ (eV)} = \frac{1240}{\lambda} \qquad (3)$$

The energy band gap value calculated from the PL spectrum was approximately 2.8 eV [15, 16]. Then the crystal size or size (diameter) is calculated from the energy gap using the Brus equation, Eq. (4):

$$E = E_g + \frac{h^2}{2d^2}\left(\frac{1}{m_e^*} + \frac{1}{m_h^*}\right) \quad (4)$$

E is the NPs band gap of 2.8 eV obtained from the PL spectrum and absorption spectrum, E_g bulk is the bulk band gap of 2.6 eV [10], m_e^* is the excited electron effective mass of 0.12 m_0, m_h^* is the excited hole effective mass of 0.8 m_0, e is the electron charge (1.6×10^{-19} Col), d is the size of NPs, m_0 is the free electron mass (9.1×10^{-31}) kg. By applying Eq. (4), the calculated NPs size was approximately 15.4 nm.

As seen in Fig. 7, UV radiation with a wavelength of 300 nm was employed. The resultant material's properties were studied by irradiating it with a wavelength of 290 nm, and a set of peaks was used in the light-generating process. However, when the sample is irradiated with a 300 nm wavelength, as shown in Fig. 7, the peak at 340 nm associated with the band-to-band transition for PbI_2 does not appear. This absence is attributed to the very low probability of this transition compared to other more prominent transitions, which are likely related to surface states induced by the nano structuring effect of PbI_2.

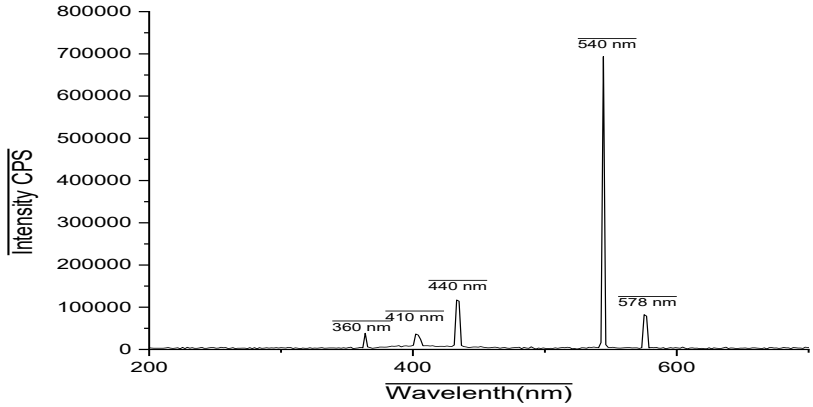

Fig.7: The PL spectrum of PbI_2: PVA excited by UV light using (300 nm).

Fig. 8 displays the photoluminescence spectrum, which was examined using the CIE 1976 chromaticity diagram. The green light generation was calculated using the following equations [17,18]:

$$u' = \frac{4X}{X + 15Y + 3Z} \quad (5)$$

$$v' = \frac{9Y}{X + 15Y + 3Z} \quad (6)$$

The symbols X, Y and Z represent the area under the curve for the three colors blue, red and green, respectively, while the two symbols u' and v' represent the chromaticity coordinates. Any color of light can be described using the chromaticity coordinates (u', v'). When they were substituted into Eqs. (5 and 6), the chromaticity of the (PbI_2: PVA) were (0.19, 0.59) and the emitted light color was green. Also, the parameters u', v' can be used to calculate the correlated

color temperature (CCT) using MacAdam's approximation algorithm with the following equations:

$$\mathrm{CCT} = -449n^3 + 3525n^2 - 6823.3n + 5520.33 \quad (7)$$

$$n = \frac{x - 0332}{y - 0.1858} \quad (8)$$

$$x = \frac{9u'}{6u' - 16v' + 12} \quad (9)$$

$$y = \frac{4v'}{6u' - 16v' + 12} \quad (10)$$

This relation is used to measure the size of nanoparticles using the Brus Eqs. (8-10) [20]. In this work, these results were used to measure the size of PbI_2 nanoparticles, providing more evidence for the results obtained from the absorption spectrum.

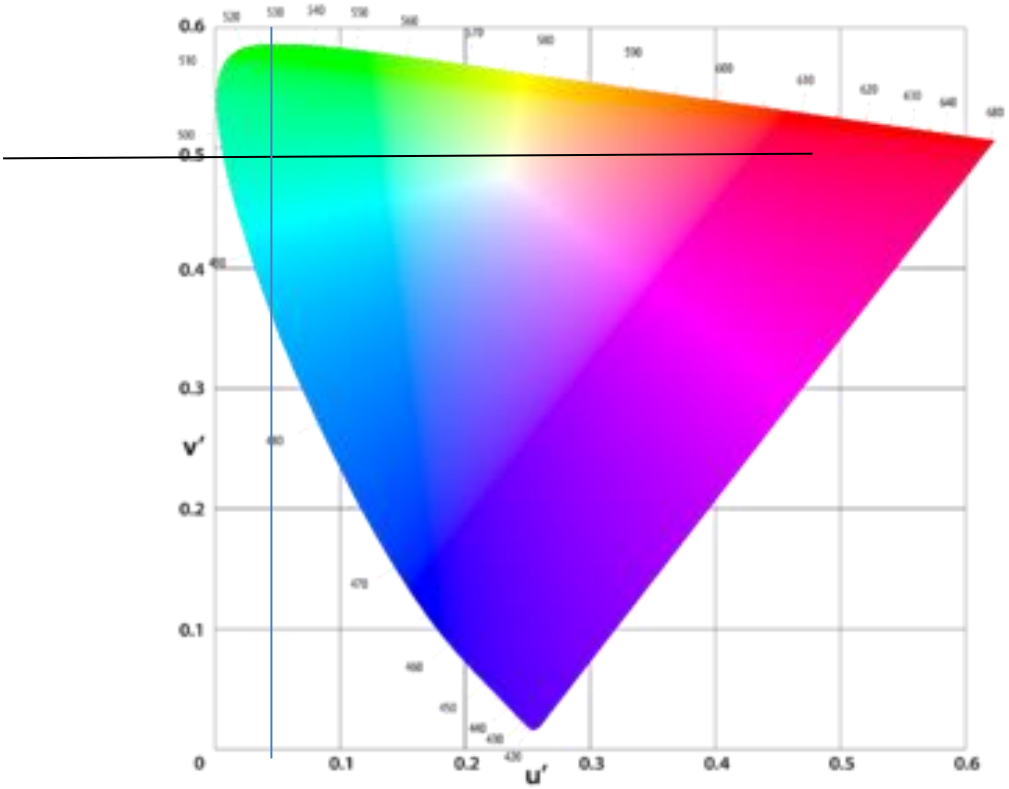

Figure 8: The CIE 1976 chromaticity diagram for PbI_2 \PVA.

The appearance of peaks due to the transitions occurring between the energy levels of both PVA and PbI_2 was observed as listed in Table 1. As shown in Fig. 9, a transition occurs between the LUMO and the valence band of PbI_2, emitting 360 and 340 nm wavelength radiation. At 340 nm, a very small peak appears, while at 360 nm, the peak is slightly larger. As for the other transitions at the 410 and 440 nm, they occur due to transitions from the conduction band to the valence band of PbI_2, corresponding to the energy gap. Note that the intensity of these peaks is somewhat weak compared to the other peaks at 540 and 578 nm, which result from the transition between the surface state (S.S.) of PbI_2 and the valence band. This surface state is significant and occurs in all materials, with its effect being greater in nanomaterials. Therefore, it was noted that

the probability of transition between the surface state and the valence band is very high, which gives the wavelength 540 nm, corresponding to the green color.

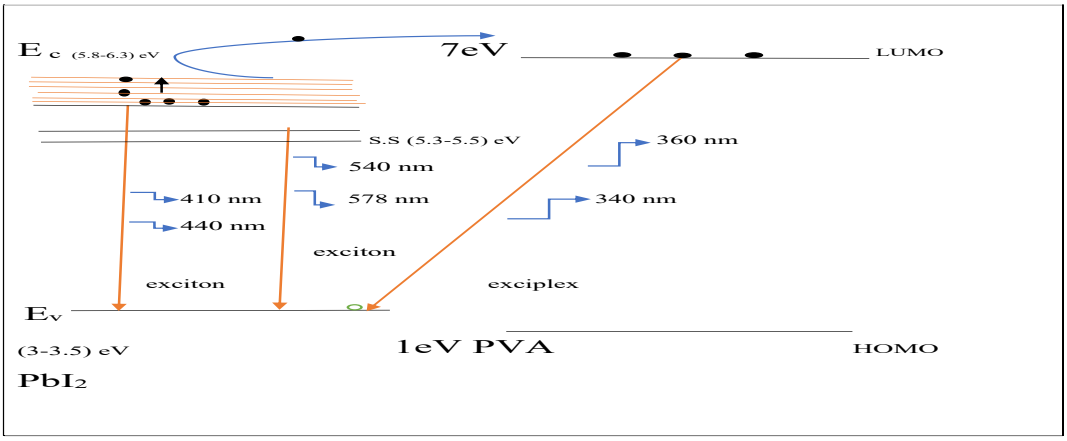

Figure 9: Energy diagram emission for PbI_2: PVA.

Table 1: The energy state of PbI_2 \ PVA.

λ (nm)	E (eV)	Transition
360 340	3.44 3.64	PVA, LUMO ➡ PbI_2, V.B
410 440	3.024 2.81	PbI_2, C. B ➡ PbI_2, V.B
540 578	2.3 2.145	PbI_2 , S.S ➡ PbI_2 , V.B

3.3. Hall Effect

The Hall effect is considered important for determining the type of semiconductor (N-type or P-type), and knowing the concentration of the charge carriers (n) is useful in calculating the Fermi wavelength. Table 2 shows the electrical properties of PbI_2 with PVA. A higher concentration of charge carriers or electrons leads to a higher efficiency of the produced light. However, so far, there has been no direct or clear relationship between intrinsically undoped semiconductors, whether n-type or p-type, and luminescence. From the Hall effect calculations, it was noted that the value of n was equal to 8.61×10^{16}, from which the Fermi wavelength was calculated, which represents the diameter of the Fermi sphere; the Fermi radius represents the dividing line between the nanostructured system and the bulk system. A size smaller than the Fermi wavelength is considered a nanostructure, meaning that the electrons are confined within the crystal, and if the crystal size is larger than the Fermi wavelength, the electrons are free, i.e., a bulk system. In this case, a nanostructure and restriction were obtained, where this restriction confines a group of electrons within the crystal, and this will generate a plasmonic resonance, where the appearance of additional peaks at 340 and 480 nm was observed, as in Fig. 6. These peaks in the fluorescence spectrum, distinct from the energy gap peaks, are due to the plasma effect. This plasmonic resonance generates energy levels that can be used for light generation at different wavelengths, with the most intense wavelength being located at 540 nm, as shown in Fig. 7.

Table 2: The electrical properties of PbI_2 with PVA.

$n(cm)^{-3}$	$R_H(cm^{-3}C^{-1})$	$s\ (o.cm)^{-1}$	$m(cm^2V^{-1}s^{-1})$	Type
8.61×10^{16}	7.25×10^{1}	3.46×10^{1}	2.51×10^{3}	P

4. Conclusions

In this work, quasi-monochromatic light was achieved by exploiting the surface states of nanomaterials. PbI_2 nanoparticles embedded in the PVA matrix exhibited strong UV absorption with efficient green photoluminescence at 540 nm. Comparison of the energy gaps obtained from absorption and PL spectra highlighted the role of indirect and surface-state transitions. At the same time, the calculated nanoparticle size agreed with optical estimations, supporting the quantum confinement effect. Hall effect analysis further confirmed the semiconducting nature of the system and its relation to light emission efficiency, demonstrating the potential of PbI_2:PVA nanocomposites for future photonic and optoelectronic applications

Conflict of Interest

The authors declare that they have no conflict of interest.

References

1. F. Yan, S. T. Tan, X. Li, and H. V. Demir, Light Generation in Lead Halide Perovskite Nanocrystals: LEDs, Color Converters, Lasers, and Other Applications, *Nano Micro Small*. **15** (47), 1902079 (2019). https://doi.org/10.1002/smll.201902079.
2. M. Mączka, J. K. Zaręba, A. Nowok, N. Sokołowski, A. Sieradzki, A. Gągor and M. Ptak, Two-Dimensional Lead Iodide Perovskites with Extremely Reduced Dielectric Confinement: Embedded Self-Erasing Second-Harmonic Generation Switching, Thermochromism, and Photoluminescence, *Chem. Mater*., **36**(21), 10758 (2024). https://doi.org/10.1021/acs.chemmater.4c02394.
3. T. Webb and S. A. Haque, *Energy Environ. Sci.*, **17**, 3244 A Comparison of Molecular Iodine Evolution on The Chemistry of Lead and Tin Perovskites (2024), https://doi.org/10.1039/D3EE03004K.
4. Y. Zhang, J. Huang, M. Zhu, Z. Zhang, K. Nie, Z. Wang, X. Liao, L. Shu, T. Tian, Z. Wang, Y. Lu and L. Fei, Significant Hydrogen Generation *Via* Photo-Mechanical Coupling in Flexible Methylammonium Lead Iodide Nanowires *Chem. Sci.*, **15**(5), 1782 (2024). https://doi.org/10.1039/d3sc05434a.
5. S. M. Mohammed, K. H. Amani, Study of the Optical and Structural Properties of PbI_2 Thin Films Prepared by Spin Coating Technique at Room Temperature, *J. Phys.: Conf. Ser.* **1795**, 012019 (2021). https://doi.org/10.1088/1742-6596/1795/1/012019.
6. L. Lanzetta, T. Webb, J. M. Marin-Beloqui, T. J. Macdonald, and S. A. Haque, Halide chemistry in tin perovskite optoelectronics: bottlenecks and opportunities, *Angewandte Chemie*, **135**(8), e202213966 (2023), https://doi.org/10.1002/ange.202213966.
7. N. G. Adnan and E. K. Hassan, Physical Properties Studies of Magnesium Phthalocyanine (MgPc) Thin Films of Different Annealing Temperatures Prepared by Pulsed Laser Deposition Technique, *Iraqi J. Phys.* **22**(3), 116 (2024). https://doi.org/10.30723/ijp.v22i3.1266.
8. A. Bouich, J. Marí-Guaita, B. M. Soucase and P. Palacios, Bright Future by Enhancing the Stability of Methylammonium Lead Triiodide Perovskites Thin Films Through Rb, Cs, and Li as Dopants, *Mater. Res. Bull.* **163**, 112213 (2023). https://doi.org/10.1016/j.materresbull.2023.112213.
9. Y. Jiang, S. He, L. Qiu, Y. Zhao, Y. Qi, Perovskite Solar Cells by Vapor Deposition Based and Assisted Methods, *Appl. Phys. Rev.* **9**(2), 021305 (2022). https://doi.org/10.1063/5.0085221.
10. A. N. Singh, A. Janna, M. Selvaraj, M. A. Asirri, S. Yun, and K. Wan Nam, *Nanomaterials*, **13**, 3049 (2023). https://doi.org/10.3390/nano13233049.
11. M. Mączka, A. Gagor, D. Stefanska, J. Hanuza, E. Kucharska, and J. K. Zareba, Divalent Methylhydrazinium-An Ultrasmall Organic Cation for Construction of Hybrid Perovskites, *Chem. Mat.* **37** (14), 5195 (2025). https://doi.org/10.1021/acs.chemmater.5c00919.
12. K. A. Khalaph, Z. J. Shanan, A. M. Jafar, and F. M. Al-Attar, Structural and Optical Properties of PbI_2 Thin Films to Fabricate Perovskite Solar Cells, *Defect and Diffus. Forum.* **398**, 140 (2020). https://doi.org/10.4028/www.scientific.net/DDF.398.140.
13. J. M. Guaita, A. Bouich, and B. Mari, Stability Improvement of Methylammonium Lead Iodide Perovskite Thin Films by Bismuth Doping, *JOM.* **74**, 3103 (2022). https://doi.org/10.1007/s11837-022-05347-4.
14. T. Hattori, T. Taira, M. Era, T. Tsutsui, S. Saito, Highly Efficient Electroluminescence from A Heterostructure Device Combined with Emissive Layered-Perovskite and an Electron-Transporting Organic Compound, *Chem. Phys. Lett.* **254**(1-2), 103 (1996). https://doi.org/10.1016/0009-2614(96)00310-7.
15. L. Gollino N. Mercier and T. Parport, Exploring Solar Cells Based on Lead- and Iodide-Deficient Halide Perovskite (d-HP) Thin Films, *Nanomater.* **13**, 1245 (2023). https://doi.org/10.3390/nano13071245.
16. N. Kumar, J. Rani, and R. Kurchania, A Review on Power Conversion Efficiency of Lead Iodide Perovskite-Based Solar Cells, *Mater. Today: Proc.* **46** (11), 5570 (2021). https://doi.org/10.1016/j.matpr.2020.09.349.

17. Z. Zheng, S. Wang, Y. Hu, Y. Rong, A. Mei, and H. Han, Development of Formamidinium Lead Iodide-Based Perovskite Solar Cells: Efficiency and Stability, *Chem. Sci.*, **13**, 2167 **(**2022). https://doi.org/10.1039/D1SC04769H.
1. Y.-T. Zeng, Z.-R. Li, S.-P. Chang, A. Ansay, Z.-H. Wang, C.-Y. Huang, Bright $CsPbBr_3$ Perovskite Nanocrystals with Improved Stability by In-Situ Zn-Doping, *Nanomater.* **12**(5), 759 (2022). https://www.mdpi.com/2079-4991/12/5/759.
2. S. Kar, N. F. Jamaludin, N. Yantara, S. G. Mhaisalkar, and W. L. Leong, Recent Advancements and Perspectives on Light Management and High Performance in Perovskite Light-Emitting Diodes, *Nanophoton.* **10**(8), 2103 (2020). https://doi.org/10.1515/nanoph-2021-0033.
3. H. A. Ashoor and A. A. Mohammed, Analysis of the electrical and optical properties of polyaniline graphene oxide metal oxide nanocomposites, *Iraqi J. Phys*. **22**(4), 27 (2024). https://doi.org/10.30723/ijp.v23i4.1241.

توليد الضوء من جسيمات نانوية من يوديد الرصاص الثنائي مضاءة بواسطة مصدر الأشعة فوق البنفسجية

شهد جاسم عبد الصاحب[1] و عمر عدنان ابراهيم[1]
[1] قسم الفيزياء، كلية العلوم، جامعة بغداد، بغداد، العراق

الخلاصة

تبحث هذه الدراسة في خصائص التألق الضوئي لجسيمات نانوية من يوديد الرصاص الثنائي (PbI_2) مدمجة في مصفوفة بولي فينيل الكحول (PVA) عند إضاءتها بالأشعة فوق البنفسجية (UV). تظهر جسيمات نانوية من يوديد الرصاص الثنائي، المنتشرة بشكل موحد داخل مصفوفة بولي فينيل الكحول، استقرارًا معززًا وانبعاثًا فعالًا للضوء بسبب البيئة الواقية التي توفرها بولي فينيل الكحول. عند الإضاءة بالأشعة فوق البنفسجية، تولد جسيمات نانوية من يوديد الرصاص الثنائي ضوءًا مرئيًا، مع تأثر خصائص الانبعاث بحجم الجسيمات النانوية وتركيزها وتفاعلها مع مصفوفة بولي فينيل الكحول. يتم تحليل دور بولي فينيل الكحول كعامل تثبيت وتأثيره على الخصائص الضوئية الفيزيائية لـ PbI_2، مما يدل على تحسن في الكفاءة الكمية والاستقرار الضوئي. يوضح نظام النانو المركب الهجين هذا التطبيقات المحتملة في الأجهزة البصرية الإلكترونية المستجيبة للأشعة فوق البنفسجية، والمواد المرنة الباعثة للضوء، وأجهزة الاستشعار الفوتونية. توفر الدراسة رؤى حول دمج جسيمات نانوية أشباه الموصلات مع مصفوفات البوليمر لتقنيات توليد الضوء المتقدمة.تستكشف هذه الدراسة التفاعل بين الاشعه فوق البنفسجية وجسيمات PbI_2 النانوية، مع التركيز على العمليات الضوئية التي تؤدي الى توليد الضوء.

الكلمات المفتاحيه: الجسيمات النانوية، التالق الضوئي، يوديد الرصاص الثنائي، بولي فاينيل الكحول، الخصائص البصرية.